Daliran, S.; Santiago-Portillo, A.; Navalón Oltra, S.; Reza Oveisi, A.; Alvaro Rodríguez, MM.; Ghorbani-Vaghei, R.; Azarifar, D.... (12-2). Cu(II)-Schiff base covalently anchored to MIL-125(Ti)-NH2 as heterogeneous catalyst for oxidation reactions. Journal of Colloid and Interface Science. 532:700-710. https://doi.org/10.1016/j.jcis.2018.07.140

Cu(II)-Schiff base covalently anchored to MIL-125(Ti)-NH_2 as heterogeneous catalyst for oxidation reactions

Andrea Santiago-Portillo,[b,†] Saba Daliran,[a,b,†] Sergio Navalón,[b,*] Ali Reza Oveisi,[c] Mercedes Álvaro,[b] Ramin Ghorbani-Vaghei,[a] Davood Azarifar,[a] Hermenegildo García[b,d,*]

[a] Faculty of Chemistry, Bu-Ali Sina University, P.O. Box: 6517838683, Hamedan, Iran

[b] Departamento de Química and Instituto de Tecnología Química CSIC-UPV, Universitat Politècnica de València, Av. de los Naranjos s/n, 46022 Valencia, Spain

[c] Department of Chemistry, University of Zabol, P.O. Box: 98615-538, Zabol, Iran

[d] Center of Excellence for Advanced Materials Research, King Abdulaziz University, Jeddah, Saudi Arabia

† Both are first author.

* Corresponding author.

Email address: sernaol@doctor.upv.es (S.Navalon); hgarcia@qim.upv.es (H.Garcia)

Abstract

MIL-125(Ti)-NH_2 has been modified by reaction of salicylaldehyde with the terephthalate amino groups to form a salicylideneimine that act as ligands of Cu^{2+}. The success of the postsynthetic modification was assessed by FTIR spectroscopy of the MIL-125(Ti)-NH_2-Sal-Cu and by analysis by ^1H NMR spectroscopy of the organic linkers upon dissolution of MIL-125(Ti)-NH_2-Sal-Cu. In comparison with parent MIL-125(Ti)-NH_2 and MIL-125(Ti)-NH_2-Sal, that exhibit a poor activity, the presence of the Cu-Schiff base complex in MIL-125(Ti)-NH_2-Sal-Cu catalyst

for the oxidation of 1-phenylethanol by *tert*-butylhydroperoxyde (TBHP, 3 eq.). Hot filtration test and reusability experiments confirm that the process is heterogeneous and that MIL-125(Ti)-NH_2-Sal-Cu is stable under the reaction conditions. Quenching studies and EPR spectra using *N*-^{t}butylphenylnitrone indicates the generation of ^{t}BuOO$^\cdot$ and ^{t}BuO$^\cdot$ under the reaction conditions. The scope of MIL-125(Ti)-NH_2-Sal-Cu as oxidation catalyst by ^{t}BuOOH was studied for benzyl alcohol as well as alicyclic and aliphatic alcohols and ethylbenzene.

Keywords: heterogeneous catalysis; metal-organic frameworks: Cu(II) Schiff-base complex; *tert*-butylhydroperoxyde

1. Introduction

Metal-organic frameworks (MOFs) or porous coordination polymers (PCPs) are a class of low-density and three-dimensional (3D) crystalline materials consisting of metal ions or clusters coordinated to rigid, multipodal organic ligands [1-3].[4] Their high surface areas (~4000 m^2/g), regular pore structures, and tunable structures and properties have made them good candidates for a variety of potential applications such as gas adsorption,[5-8] separation,[9-12] catalysis,[13-23] sensing,[24] drug delivery,[25] photocatalysis,[26] and environmental remediation, among other possibilities.[27]

Post-synthetic modification (PSM) of MOFs, enables chemists to incorporate the new functionalities into the frameworks, adapting the properties of these solvents for diverse applications.[28,29] MIL-125(Ti)-NH_2 (MIL = Materials of Institute Lavoisier), a porous titanium-based MOF [$Ti_8O_8(OH)_4$(bdc-NH_2)$_6$, bdc-NH_2 = 2-amino-1,4-benzenedicarboxylate], has a quasi-cubic tetragonal structure comprised of amino-dicarboxylate linkers connected to octameric $Ti_8O_8(OH)_4$ oxo-clusters. The framework contains octahedral and tetrahedral cages of ~12.5 Å and ~6.1 Å in diameter, respectively, accessible through triangular windows (5-7 Å) (Figure 1).[30-33] There have been some reports relating the applications of the MOF in photocatalytic and catalytic oxidation reactions such as the photocatalytic aerobic oxidation of aromatic alcohols and the conversion of *N*-hydroxy-carbamates into *N*-hydroxy-oxazolidinones,[34,35] and H_2 production.[12] Specifically, MIL-125(Ti) has been used as selective oxidation catalyst for the oxidative desulfuration and for the conversion of alkylphenols to the corresponding *p*-benzoquinones.[36-38] However, there are no report documenting a multifunctionality Ti–based MOF in catalytic oxidations using TBHP. Recently, MIL-53(Al)-NH_2 solid has been functionalized with salicylaldehyde and further metalized with Cu^{2+} to form

the Schiff base complex and this material used as catalyst for oxidation of styrene and cyclohexene using TBHP.[39] Although this precedent was focused only on the oxidation of two alkenes, it was found that MIL-53(Al)-NH_2-Sal Cu deactivates in the first use from 98 to 87 % conversion for styrene oxidation using TBHP. This fact was attributed to the occurrence of Cu leaching in a measurable extent, although it would have been convenient to confirm the structural stability of the MIL-53 (Al)-NH_2 by XRD. In addition considering the flexibility of the MIL-53 structure that can be present in a conformation of closed pores as well as the 1D geometry of its pores, it becomes apparent that this MOF structure could not the best suited for catalysis compared to rigid, open pore, 3D structures of other different MOFs such as MIL-125 (Ti).[39]

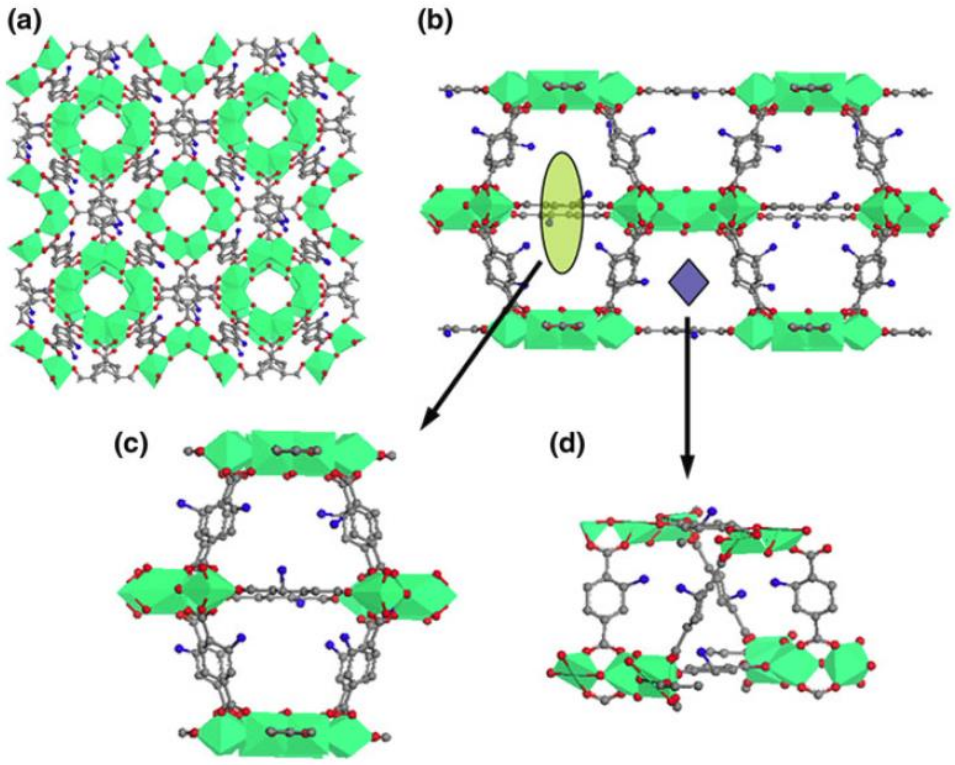

Figure 1. (a) Perspective view of NH_2-MIL-125(Ti) with a central octameric Ti_8 cluster surrounded by 12 others. (b) 3D structure of NH_2-MIL-125(Ti); the yellow oval and purple

square indicate the octahedral and the tetrahedral pores, respectively. (c) Ball and stick representation of the octahedral (c) and tetrahedral (d) cages. The color code is as follows: carbon, gray; oxygen, red; nitrogen, blue; titanium, green (taken with permission from ref. [33])

In this article we describe a synthetic strategy to prepare a novel multifunctional Ti–based MOF, namely MIL-125(Ti)-NH_2-Sal-Cu, via PSM of the amine-functionalized Ti-based MOF in two steps; I) imine formation reaction and II) metalation with copper, targeting the development of a highly efficient heterogeneous catalyst for the oxidation of benzylic compounds using *tert*-butyl hydroperoxide (TBHP) as terminal oxidant. The incorporation of Cu into the MOF, can result in creation of new active sites, thereby increasing its catalytic activity.

2. Experimental section

Materials. All reagents were purchased from Sigma-Aldrich and used without further purification.

Characterization. X-ray diffractograms were recorded using a Philips Xpert diffractometer equipped with a graphite monochromator (40 kV and 45 mA) employing Ni filtered Cu Kα radiation. ATR-FTIR spectra of room temperature equilibrated samples were recorded by using a Bruker Tensor 27 instrument. The N_2 adsorption isotherms at 77 K were measured using an ASAP 2010 Micrometrics Instrument Corp., USA. The samples were degassed in vacuum at 150 °C for 12 h and then measured at 77 K. X-ray photoelectron (XP) spectra were recorded on a SPECS spectrometer with a MCD-9 detector using a monochromatic Al (Kα= 1486.6 eV) X-ray source. Spectra deconvolution was performed with the CASA software using the C 1s peak at 284.4 eV as binding energy reference.[40] A scanning electron microscope (SEM, Zeiss instrument, AURIGA Compact) has been employed to determine the morphology of the solid samples. Metal (Cu, Ti) contents were determined using inductively coupled plasma atomic

emission spectroscopy (ICP-AES, Perkin-Elmer). Before ICP-AES analyses, the samples (5 mg) were digested in conc. H_2SO_4:30% aq. H_2O_2 (3:1 v/v). The clear solution was then diluted to 25 mL with deionized H_2O and analyzed via ICP-AES. Liquid phase ^{1}H-NMR spectra were recorded in a Bruker Advance 400 MHz. EPR spectra using BPN as spin trap were carried out as follows: catalyst (100 mg L^{-1}), BPN (1,000 mg L^{-1}), H_2O_2 to BPN molar ratio 1, pH 4, artificial solar light irradiation, reaction time 5 min. EPR spectra were recorded on a Bruker EMX spectrometer using the following settings: frequency 9.803 GHz, sweep width 3489.9 G, time constant 40.95 ms, modulation frequency 100 kHz, modulation width 1 G, microwave power 19.92 mW.

Preparation of MIL-125(Ti)-NH_2

MIL-125(Ti)-NH_2 was prepared according to the literature.[12] Briefly, 2-aminoterephthalic acid (1.43 g) was dissolved in a mixture of dry DMF (40 mL) and dry methanol (10 mL) at room temperature and the mixture was sonicated for 10 min. Then, 1.43 mL of titanium isopropoxide was added and the resulting mixture was transferred to a Teflon container inserted in a stainless autoclave. The sealed autoclave was heated at 110 ºC for 72 h. The solid obtained was filtered and washed with DMF at room temperature and, then, with hot DMF overnight. This washing procedure was repeated using methanol as solvent. Finally, the solid was dried at 100 ºC under air.

Preparation of MIL-125(Ti)-NH_2-Sal

In a round-bottomed flask MIL-125(Ti)-NH_2 (1 g) was stirred in acetonitrile (35 mL) for 20 min. Then, salicylaldehyde (5 mmol) was added to the resultant suspension, and the flask was sealed and stirred in an oil bath at 40 °C for 72h. After this time, the solution was cooled to room

temperature, and the precipitate was removed by centrifugation. The obtained solid was washed with acetonitrile (three times) and anhydrous methanol (three times). Finally, the obtained MIL-125(Ti)-NH_2-Sal crystals were dried under vacuum oven at 80 °C for 12 h.

Preparation of MIL-125(Ti)-NH_2-Sal-Cu

The as-prepared MIL-125(Ti)-NH_2-Sal (1.2 g) and $CuCl_2$ (0.6 mmol) were dispersed into absolute ethanol (20 mL), and the mixture was stirred at 40 ºC for 24 h. The obtained crystals were centrifuged, washed with absolute ethanol (several times) followed by drying overnight under vacuum at 80 °C.

Catalytic Experiments

Typically, 10 mg of catalyst, previously dried in an oven at 100 ºC, was added to a round-bottom flask (25 mL) containing CH_3CN as solvent (5 mL) and the corresponding substrate (1 mmol) together with the required amount of TBHP (i.e. 3 eq. respect to the substrate). Subsequently, the reaction mixture was placed in a preheated bath at 80 ºC and magnetically stirred. In the case of the reaction at 5 bar of O_2, the reaction takes place in a reactor at 100 ºC.

Selective quenching experiments with DMSO and *p*-benzoquinone were carried out as described above, but in the presence of 20 mol % of these quenchers respect to the substrate.

The progress of the reaction was followed by gas chromatography (GC) using a flame ionization detector. Aliquots of reaction mixture at different times were diluted in CH_3CN and a known amount of external standard was added. Quantification was carried by using calibration curves of commercial for available samples.

3. Result and Discussion

3.1. Characterization of the multifunctional MOF (MIL-125(Ti)-NH_2-Sal-Cu)

MIL-125(Ti)-NH_2-Sal-Cu was prepared through a two-step PSM route starting from MIL-125(Ti)-NH_2 according to Scheme 1. Firstly, MIL-125(Ti)-NH_2 was prepared by solvothermal synthesis using 2-aminoterephtalic acid and Ti(O^iPr)$_4$ as precursors as previously reported. Then, MIL-125(Ti)-NH_2-Sal was prepared by reaction MIL-125(Ti)-NH_2 and salicylaldehyde leading to the formation of the corresponding imine (Schiff base). Finally, MIL-125(Ti)-NH_2-Sal was metallated using an ethanolic Cu(II) solution leading to the formation of MIL-125(Ti)-NH_2-Sal-Cu.

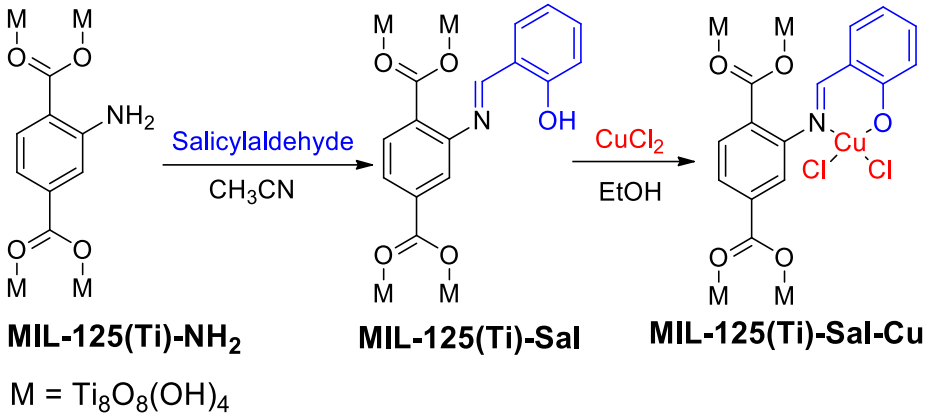

Scheme 1. Schematic preparation of MIL-125(Ti)-NH_2-Sal-Cu.

PXRD of the three prepared MOFs showed that the three samples are isostructural to the pattern MIL-125(Ti)[30-32,41] and their crystallinity is maintained after the PSM steps (Figure 2a). The intense peaks at 2θ 6.8, 9.5, and 11.6º are related, respectively, to the (*101*), (*200*), and (*211*) Miller planes as reported for MIL-125 (Ti)-NH_2.[31]

MIL-125(Ti)-NH_2 characterization and further functionalization with salicylaldehyde with or without Cu(II) metalation was established by spectroscopic and analytical techniques. FT-IR spectrum of MIL-125(Ti)-NH_2 (Figure 2b) shows the expected symmetric stretching and

asymmetric vibrations of the $–NH_2$ group at about 3,300 cm^{-1}, the carbonyl band of the carboxylate at about 1630 cm^{-1} along with the C-N and C-O stretching vibrations in the region between 1200 and 1400 cm^{-1}. The bands in the region of 1650–1400 cm^{-1} can be attributed to the carboxylate coordinated to Ti–oxo cluster of the MOFs. Ti-O vibrations appear in the region between 700 and 400 cm^{-1}. FT-IR spectrum of MIL-125(Ti)-NH_2-Sal (Figure 2b) shows the salicylidene imine formation as revealed by the following features: i) the appearance of the new peak at 1571 cm^{-1} (C=N bond) along with the decrease two bands of amine group of the parent MIL-125(Ti)-NH_2 around 3460 cm^{-1} and 3342 cm^{-1} and ii) the new absorption band around 653 cm^{-1} attributable to the C(sp^2)-OH bond in the salicylidene imine (Sal group) in the MIL-125(Ti)- NH_2-Sal materials. After the post-synthetic metalation, the copper-nitrogen and copper-oxygen peaks at about 630 and 510 cm^{-1} are not observed (Figure 2b). The bands are probably very week[42,43] or overlapped with the Ti-O-Ti-O vibrations.

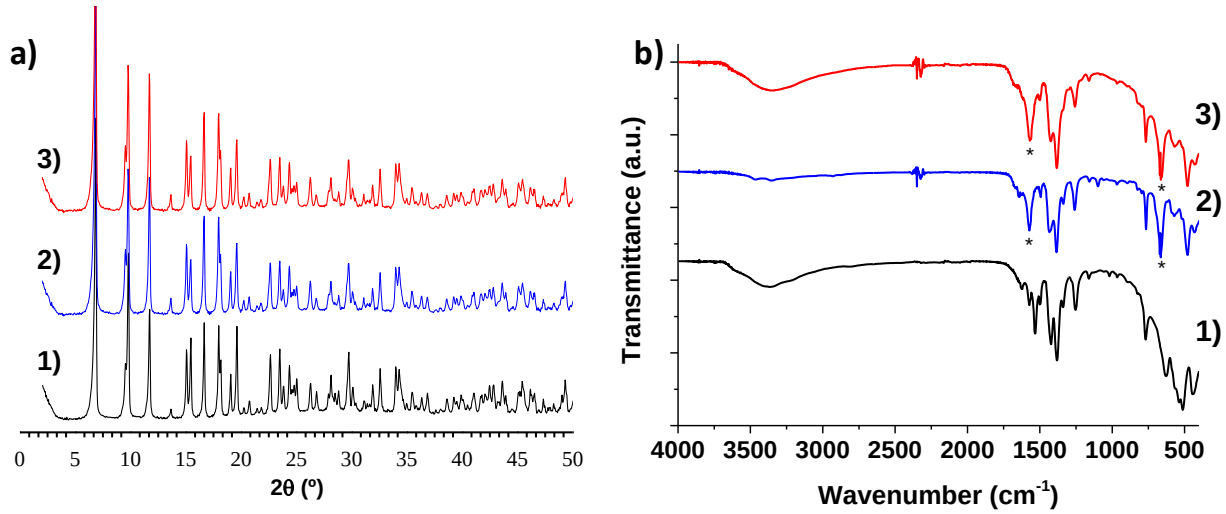

Figure. 2. PXRD patterns (a) and FT-IR spectra (b) of MIL-125(Ti)-NH_2 (1), MIL-125(Ti)- NH_2-Sal (2) and MIL-125(Ti)- NH_2-Sal-Cu (3). Legend 1b: the asterisks indicate the C=N and C(sp^2)-OH functional groups present in the MOF.

The functionalization of MIL-125(Ti)-NH_2 with salicylaldehyde was further investigated by ^{1}H-NMR spectroscopy upon digestion of MIL-125(Ti)-NH_2 and MIL-125(Ti)- NH_2-Sal in acidic conditions (HF in d_6-DMSO) as depicted in Figure 3. The results confirmed the successful functionalization of MIL-125(Ti)-NH_2 with salicylaldehyde by the appearance of new proton signals (7.65 ppm, dd, J = 7.8 and 1.6 Hz, 1H; 7.53-7.48 ppm, m, 1H; 7.00-6.93 ppm, m, 2H). In addition, the percentage of MIL-125(Ti)-NH_2 functionalization by salicylaldehyde was estimated to be 15% from ^{1}H-NMR spectroscopy. ICP–OES analysis of the digested MIL-125 (Ti)-Sal-Cu showed a copper loading of 4.1 wt%. This copper loading in the MIL-125(Ti)- NH_2-Sal-Cu solid corresponds to a Ti/Cu ratio of about 6:1 and about 1.3 copper ions per octa-titanium node.

NH_2-MIL-125(Ti) [$Ti_8O_8(OH)_4(O_2C\text{-}C_6H_3NH_2\text{-}CO_2)_6$] after about 15% functionalization give MIL-125 (Ti)-Sal [Estimated formula based on ^{1}H NMR: $Ti_8O_8(OH)_4(O_2C\text{-}C_6H_3NH_2\text{-}CO_2)_5(C_{15}H_9NO_5)_1$] and after that MIL-125 (Ti)-Sal-Cu [Estimated formula based on previous formula: $Ti_8O_8(OH)_4(O_2C\text{-}C_6H_3NH_2\text{-}CO_2)_5(C_{15}H_8Cl_2CuNO_5)_1$. The Calculated ICP-OES (%) of MIL-125 (Ti)-Sal-Cu showed a copper loading of ~3.5 wt%.

Attempts to establish by ^{1}H-NMR spectroscopy formation of the Cu Schiff base were unsuccessful, since only the ^{1}H-NMR spectra of MIL-125(Ti)-NH_2-Sal could be recorded. Apparently the presence of diamagnetic Cu species makes impossible recording analogous ^{1}H NMR spectrum of MIL-125(Ti)-NH_2-Sal-Cu. On the other hand, in order to minimize the percentage of Cu^{2+} that could be attached to the material through hydroxyl groups on the MOF node,[44] the solid was thoroughly washed to remove as much as possible this adventitious Cu.

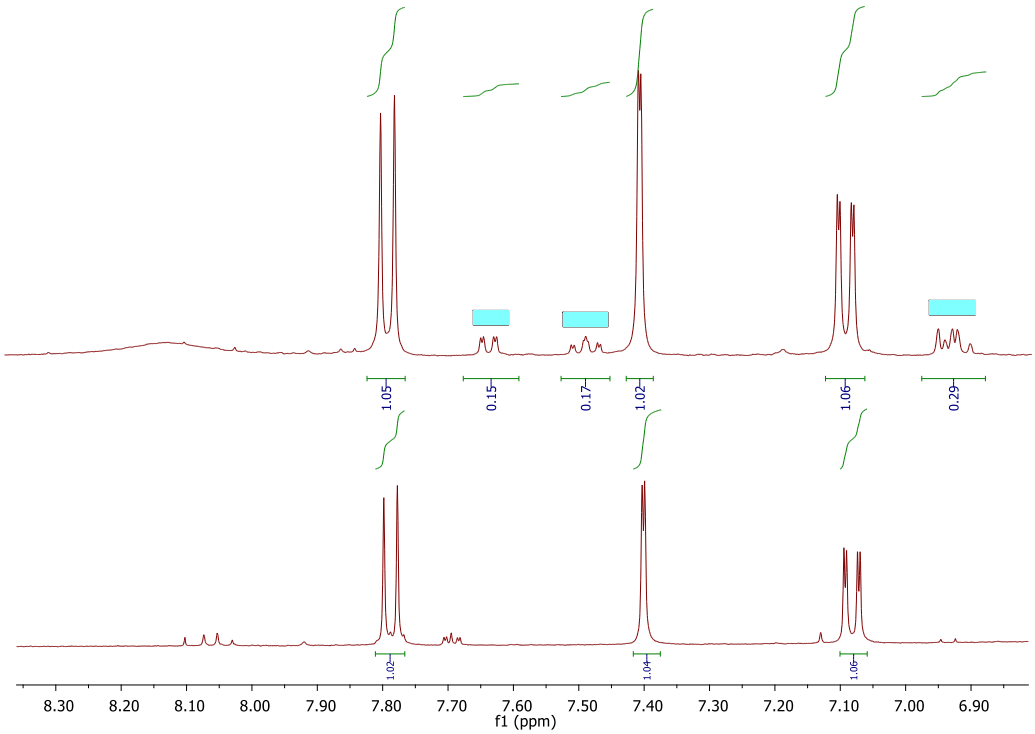

Figure 3. ^{1}H-NMR spectra in the region between 6.8 and 8.4 ppm of digested MIL-125(Ti)-NH_2 (bottom) and MIL-125(Ti)- NH_2-Sal (top) solids in HF (DMSO-d_6); rectangular shapes (□) are the new peaks. The residue peaks at around 8.1, 7.7, and 7.12 ppm in ^{1}H NMR of digested MIL-125(Ti)-NH_2 could correspond to the partial protonation (during the digestion process) and/or formylation of the linker during the synthesis in DMF.[45]

XPS analysis was also employed for the characterization of the three Ti-based MOFs (Figure 4).[46] C1s clearly shows the characteristic C=C and C-H signals appearing at 284.4 eV together with the O-C=O bonds at about 289 eV for the three solids (Figure 4a), corresponding to the amino terephthalate ligand. Functionalization of MIL-125(Ti)-NH_2 with salicylaldehyde with or without copper metalation leads to additional C1s bands (C=N and C-O) that overlap with that of the parent MIL-125(Ti)-NH_2 organic ligand. Interestingly, these C-O and C=N bands are more clearly observed in the XPS O1s and N1s peaks, respectively (Figure 4b and 4c). As expected

similar XPS Ti 2p signals were recorded for the three MIL-125 Ti-based MOFs (Figure 4d). In the case of the MIL-125(Ti)- NH_2-Sal-Cu sample the corresponding Cu(II) signals in the XPS Cu 2p also were observed (Figure 4e). Figure S1 shows the XPS deconvolution of the different elements present in the MIL-125(Ti)- NH_2-Sal-Cu material.

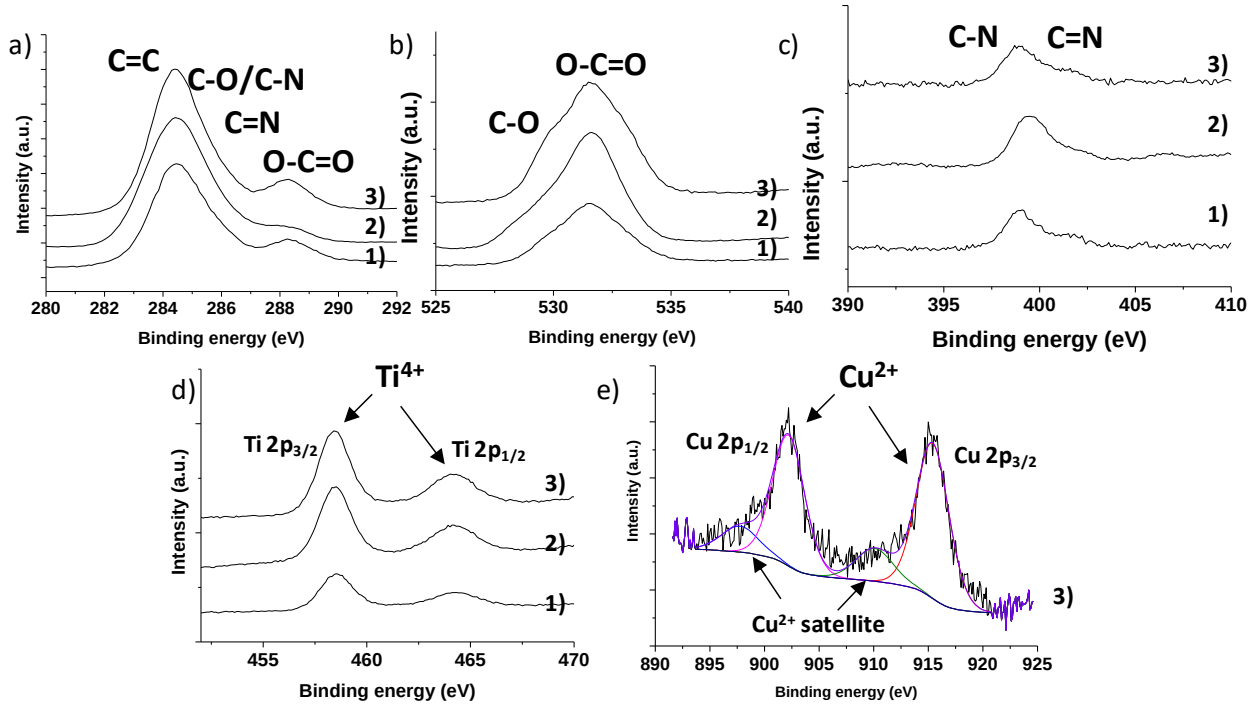

Figure 4. XPS of MIL-125(Ti)-NH_2 (1), MIL-125(Ti)- NH_2-Sal (2) and MIL-125(Ti)- NH_2-Sal-Cu. Legend: a) C 1s; b) O 1s; c) N 1s; d) Ti 2p; e) Cu 2p

N_2 adsorption-desorption experiments at 77 K were used to determine the BET surface area of 1215, 1045, and 958 m^2/g, and the pore volume of 0.9, 0.8, and 0.6 cm^3/g for the prepared MIL-125(Ti)-NH_2, MIL-125(Ti)-NH_2-Sal, and MIL-125(Ti)-NH_2-Sal-Cu MOFs, respectively (Figures S2-S4). The gradual reduction of both BET surface area and pore volume from MIL-125(Ti)-NH_2 to MIL-125(Ti)-NH_2-Sal, and to MIL-125(Ti)-NH_2-Sal-Cu was in accordance with the partial pore filling of the parent MOF with the salicylaldehyde moiety with or without Cu(II)

ions. N_2 adsorption isotherm of MIL-125(Ti)-NH_2-Sal-Cu is typical of type I, as previous reported for the parent MOF,[30-32] MIL-125(Ti)-NH_2 (Figure S4).

The morphology of the MIL-125(Ti) particles was assessed by SEM measurements (Figure 5). The three MIL-125(Ti) based MOFs prepared in this work show particles with sizes ranging between 300 and 800 nm although in the case of MIL-125(Ti)-NH_2-Sal-Cu also smaller particles were observed. The disk-like morphology and the average particle size is similar to that previously reported for MIL-125(Ti)-NH_2.[46]

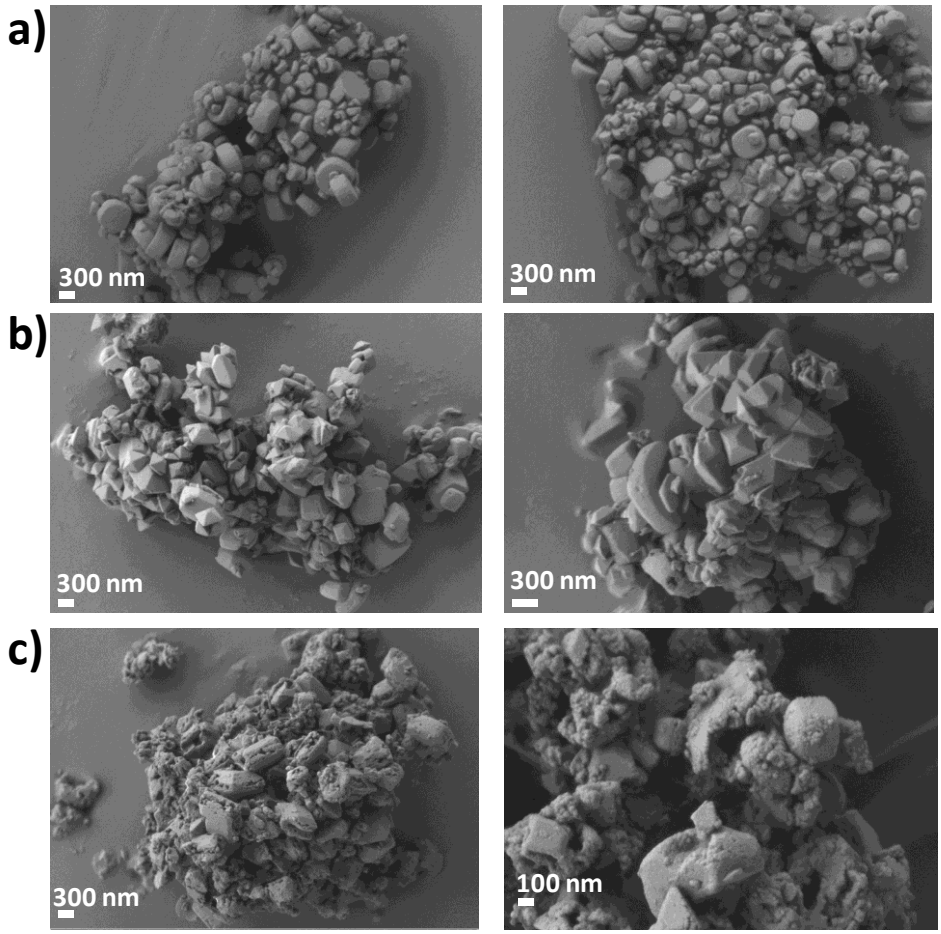

Figure 5. Representative SEM images of MIL-125(Ti)-NH2 (a), MIL-125(Ti)-NH_2-Sal (b) and MIL-125(Ti)-NH_2-Sal-Cu.

3.2. Catalytic activity

The catalytic activity of MIL-125(Ti)-NH_2-Sal-Cu was initially checked for the aerobic oxidation of 1-phenylethanol, but all the attempts failed. Subsequent studies were carried out using an excess of tert-butyl hydroperoxide (TBHP) respect to the substrate. A TBHP to 1-phenylethanol molar ratio of 3 was found to give the optimal performance for the oxidation. Control experiments under the same conditions using MIL-125(Ti)-NH_2 or MIL-125(Ti)-NH_2-Sal indicate that the main active site of the reaction is the salicylideneimine-Cu(II) complex moiety (Sal-Cu) in the MIL-125(Ti)-NH_2 material. Figure 6 shows the time-conversion plot for 1-phenylethanol oxidation by TBHP under some representative conditions. The only product observed was acetophenone reaching high conversions, about 99 %, with almost complete selectivity.

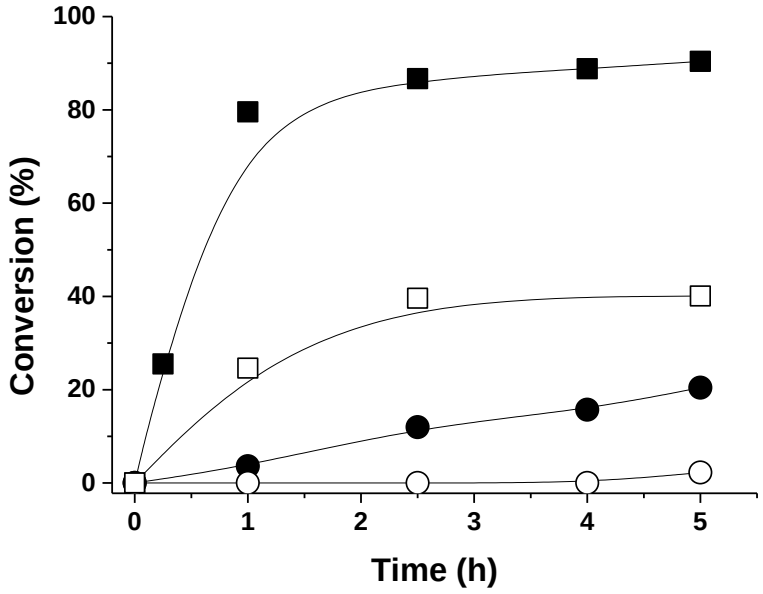

Figure 6. Time-conversion plot for the oxidation of 1-phenylethanol to acetophenone with TBHP using MIL-125(Ti)-NH_2-Sal-Cu (■), MIL-125(Ti)-NH_2-Sal (□) and MIL-125(Ti)-NH_2 (●). A blank control in the absence of catalyst is also presented (○). Reaction conditions: Catalyst (10 mg), substrate (1 mmol), CH_3CN (5 mL), TBHP (3 eq.) and 80 ºC.

Catalyst stability was studied by performing consecutive uses of the same sample, determining time-conversion plots for each run and studying the crystallinity of MIL-125(Ti)-NH_2-Sal-Cu after five consecutive uses (Figure 7a). As it can be seen there, not changes in the initial reaction rate, final conversion, selectivity and temporal evolution of the reaction were observed in the five runs. Furthermore, XRD of the fresh, one time, three and five times used materials were coincident indicating that the crystallinity of the sample is preserved under the reaction conditions (Figure 7b). All these data indicate that the catalyst is stable under the conditions of the TBHP oxidation.

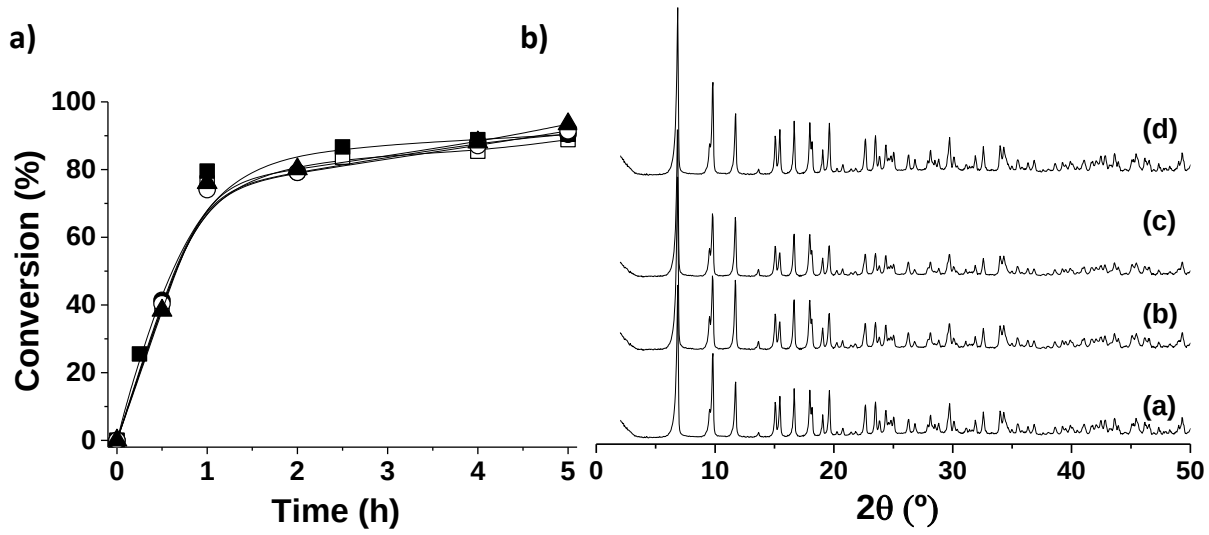

Figure 7. a) Time-conversion plots for the oxidation of 1-phenylethanol to acetophenone with TBHP using MIL-125(Ti)-NH_2-Sal-Cu as catalyst. Legend: First use (■), second (□), third (●), fourth (○) and fifth use (▲). **b)** XRD Pattern of MIL-125 (Ti)-NH_2-Sal-Cu fresh (a), after the first use (b), after the third use (c) and after the fifth use (d). Reaction conditions: Catalyst (10 mg), substrate (1 mmol), CH_3CN (5 mL), TBHP (3 eq.) and 80 ºC.

Stability of MIL-125 (Ti)-NH_2-Sal-Cu was also confirmed by performing a productivity test. In this experiment a large excess of substrate is used employing a minimal amount of catalyst. The results

are presented in Figure 8. As it can be seen there, only 2 mg of MIL-125 (Ti)-NH_2-Sal-Cu catalyst was able to convert completely 5 mmol of substrate. Thus, a minimum TON value of 4200 cycles per Cu atom was achieved.

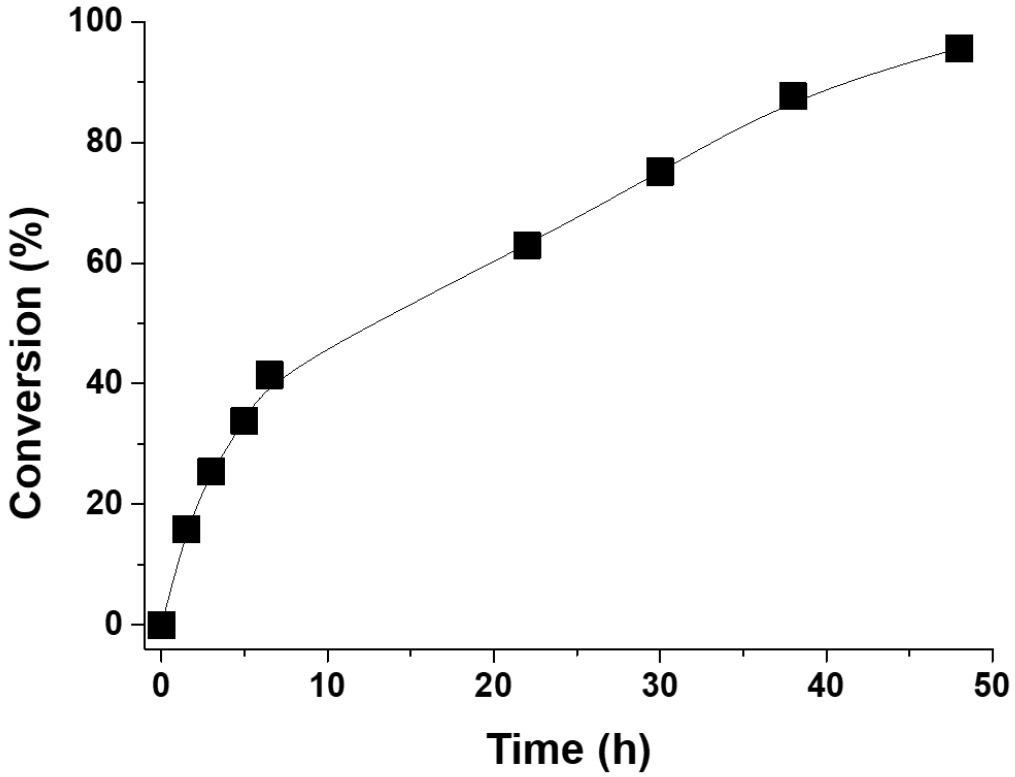

Figure 8. Time-conversion plots for the productivity test of the oxidation of 1-phenylethanol to acetophenone with TBHP using MIL-125(Ti)-NH_2-Sal-Cu as catalyst (■). Reaction conditions: Catalyst (2 mg), substrate (5 mmol), CH_3CN (25 mL), TBHP (3 eq.) and 80 ºC**.**

Heterogeneity of the process was assessed by carrying out two twin experiments in which in one of them the solid catalyst was filtered at 20 min reaction time, when conversion was about 30 %, and allowing the reaction to continue in the absence of any solid (Figure 9a). It can be

seen that the progress in the absence of catalyst was very minor, while about 50 % of the further conversion increase was observed for the twin experiment in where the catalyst was not filtered during the reaction. ICP-OES analysis reveal a titanium and copper leaching less than 0.02 and 1 wt%, respectively of the initial metal present in the MIL-125(Ti)-NH_2-Sal-Cu catalyst. To understand that in the hot filtration test the reaction progress is very small even though Cu species are present, it can be proposed that the leached Cu species are probably devoid of significant catalytic activity. It is very likely that the oxidizing conditions of the reactions lead to the formation of Cu oxides that are considerably less active than Cu-Sal complexes.

Two control experiments using $CuCl_2$ and Cu-Sal as homogeneous catalysts in the amount of copper leached from the solid to the solution show conversions lower than 40% (Figure 9a). The relatively similar time-conversion plots measured for $CuCl_2$, regardless its amount, could indicate either decomposition of TBHP or aggregation of Cu species (probably as oxides). In any case, it is clear that the activity of $CuCl_2$ in homogeneous phase does not follow a linear relationship with the amount of $CuCl_2$. Importantly, the catalytic activity is higher when using MIL-125(Ti)-NH_2-Sal-Cu as catalyst respect to the use of the same copper amount in the form of $CuCl_2$ salt as homogeneous catalyst (Figure 9a). The fact that Cu-Sal in homogeneous phase performs as catalyst significantly worse than the same complex immobilized in the framework of MIL-125(Ti)-NH_2 shows the advantages of immobilization of this Schiff base complex into the structure of a porous material. Similar observation had been previously reported in the literature and attributed to a much faster deactivation pathway for the soluble complex, for instance forming μ-oxo dimers, than when these complexes are attached to a rigid framework where dimerization is precluded.[47,48]

The use of TiO_2 as heterogeneous catalyst with the amount found in the leaching resulted in a conversion of 1-phenylethanol of less than 15 % after 5 h.

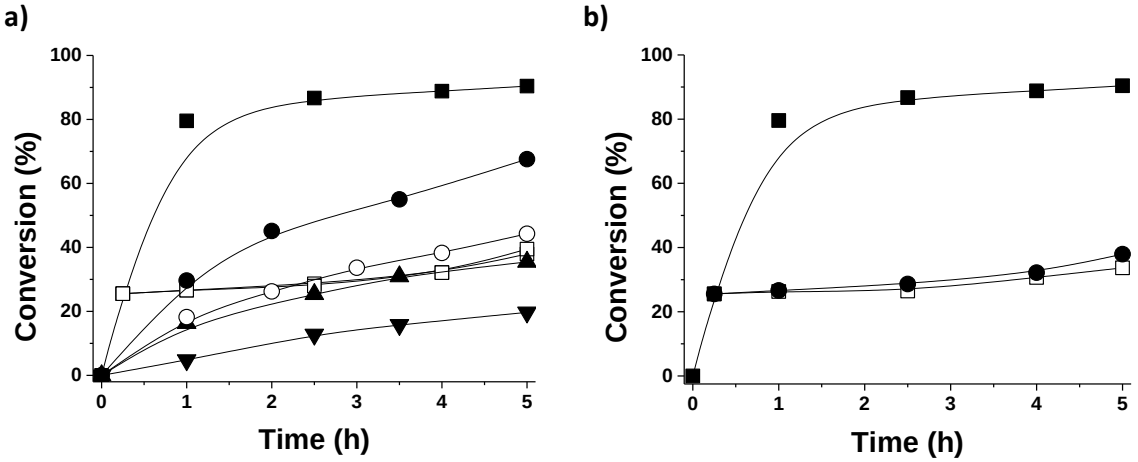

Figure 9. a) Time-conversion plots for the oxidation of 1-phenylethanol to acetophenone with TBHP using MIL-125(Ti)-NH_2-Sal-Cu as catalyst (■) and when the catalyst is filtered at 20 min (□). Blank control experiments using $CuCl_2$ as homogeneous catalyst with the same amount of copper than that present in MIL-125-Sal-Cu (▲) and that found in the leaching measurements (▼), with Cu-Sal as catalyst with the same amount of copper than that present in MIL-125-NH_2-Sal-Cu (○) and with MIL-125(Ti)-NH_2-Cu with the same amount of copper than that present in MIL-125-NH_2-Sal-Cu (●). Reaction conditions: Catalyst (10 mg), substrate (1 mmol), CH_3CN (5 mL), TBHP (3 eq.) and 80 ºC**. b)** Time-conversion plot for the oxidation of 1-phenylethanol to acetophenone with TBHP using MIL-125(Ti)-NH_2-Sal-Cu as catalyst (■) and after adding at 20 min a 20 mmol % of *p*-benzoquinone (□) and 20 mmol% of DMSO (●). Reaction conditions: Catalyst (10 mg), substrate (1 mmol), CH_3CN (5 mL), TBHP (3 eq.) and 80ºC.

Since the absence of Cu species others than Cu-Sal cannot be completely excluded and in order to address their possible role, an additional control using MIL-125(Ti)-NH_2-Cu, in where Cu^{2+} should be interacting with amino or hydroxyl groups of the framework, was also performed. This material was prepared by impregnation of MIL-125(Ti)-NH_2 with the amount of $CuCl_2$

present in MIL-125(Ti)-NH_2-Sal-Cu complexes. The results are present in Figure 9. As it can be seen there, and in accordance with the well-known catalytic activity of Cu-Sal respect to $CuCl_2$, the activity of MIL-125(Ti)-NH_2-Cu was much lower than that of MIL-125(Ti)-NH_2-Sal-Cu, indicating that the contribution of adventitious Cu species not forming Cu-Sal complexes should be much lower than that of the Cu-Sal complex.

To put into context the catalytic activity of MIL-125 (Ti)-NH_2-Sal-Cu respect to some other catalysts reported for the same reaction, Table 1 collects reported TON values and the number of cycles achieved with MIL-125 (Ti)-NH_2-Sal-Cu for 1-phenylethanol oxidation.

Table 1. Oxidation of 1-phenylethanol to acetophenone using different catalysts.

Catalysts	TON	Ref.
MIL-125(Ti)-NH_2-Sal-Cu	4200	This work
TiO_2	25	This work
Oxo-vanadium Schiff anchored on mesoporous silica	50	49
Water-soluble copper complex based on $CuCl_2$ and 2,2-biquinoline-4,4-dicarboxylic acid dipotassium salt	40	50
Palladacycle based on 2-phenylpyridine	130	51

The reaction mechanism, and particularly the nature of the active species involved in alcohol oxidation, was studied by carrying out the oxidation of 1-phenylethanol in the presence

of some radical quenchers, namely *p*-benzoquinone and DMSO. It is known that *p*-benzoquinone is a selective quencher of superoxide and peroxyl radicals, while DMSO is selective for oxyl radicals including hydroxyls ($OH^{\cdot}$). The results achieved are presented in Figure 9b. It was observed that upon addition of any of these two quenchers at 20 min reaction time, the progress of the reaction stops completely. These indicates that both types of species peroxyl and alcoxyl radicals are involved in the reaction in the same extent, one way to reconcile these apparently contradictory data from the quenching study is to assume that the real active species causing alcohol oxidation are tert-butoxyl radicals, but the precursor of these hydroxyl radicals are $^{t}BuOO^{\cdot}$ radicals. In this way, considering the consecutive participation of the two different oxygen center radicals, one being the precursor of the other, interception of one of the two intermediates would lead to the same influence on the alcohol oxidation, resulting in the complete quenching of the reaction. These radical species can be formed at the Cu-Sal complex in MIL-125 (Ti)-NH_2 by cleavage of TBHP.

To get spectroscopic evidence on the generation of any of these $^{t}BuOO^{\cdot}$ and $^{t}BuO^{\cdot}$ radicals, EPR spectra using a spin trapping agent were carried out. EPR measurements using PBN as spin trap showed that the presence of MIL-125(Ti)-NH_2-Sal-Cu generates high concentration of radicals, compared to the blank experiment at the same time (Figure 10 a). The experimental EPR spectrum could be simulated adequately by using the reported hyperfine coupling constants for the PBN-O-$OC(CH_3)_3$ adduct. Furthermore, a remarkable good fitting of the experimental EPR spectrum was achieved when to the theoretical EPR spectrum of the PBN adducts was refined by adding a minute percentage of PBN-O-$OC(CH_3)_3$. Therefore, according of these EPR spectra, both, *tert*-butylperoxy and *tert*-butyloxy radicals are generated mainly by action of Cu-Sal.

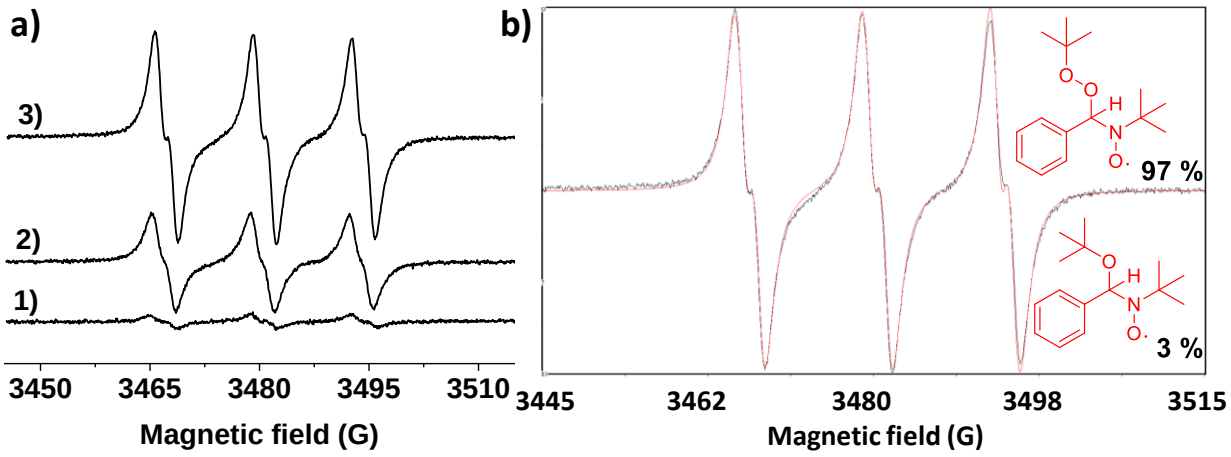

Figure 10. a) Experimental EPR spectra in CH_3CN as solvent at 70 ºC using (1) PBN + TBHP for 10 min, PBN + TBHP + MIL-125(Ti)-NH_2-Sal-Cu for 5 (2) and 10 (3) min. b) Experimental (spectrum 3 in panel a) and simulated EPR spectra for a mixture of 97% of PBN-$OOC(CH_3)_3$ and 3% of PBN-$OC(CH_3)_3$. Hyperfine coupling constants of PBN-$OOC(CH_3)_3$ (AG_N = 13.45 and AG_H = 1.7) and PBN-$OC(CH_3)_3$ (AG_N = 13.62 and AG_H = 1.72).

These results agree very well with the quenching experiments showing that the two species participate in 1-phenylethanol oxidation. Considering the relative activity of both oxygen radicals it is more likely that $(CH_3)_3COO^{\cdot}$ is the precursor of the most reactive $(CH_3)_3CO^{\cdot}$ that will be ultimately responsible for alcohol oxidation.

Scheme 2 shows a plausible reaction mechanism for TBHP activation using MIL-125(Ti)-NH_2-Sal-Cu as heterogeneous catalyst. It is proposed that Cu(II) can act as redox or Lewis center binding to the Cu^{2+} ion forming a metal-peroxo species. Subsequent homolytic Cu-O bond breaking will lead to Cu (I) and $^tBuOO^{\cdot}$ radicals. These $^tBuOO^{\cdot}$ radicals are, according to EPR, the most abundant intermediates and can form the most reactive, active $^tBuO^{\cdot}$ oxyl radical, for instance, by dimerization of two $^tBuOO^{\cdot}$ radicals and subsequent oxygen evolution. The catalytic cycle will be close by Cu (I) to Cu (II) reoxidation by $^tBuOO^{\cdot}$.

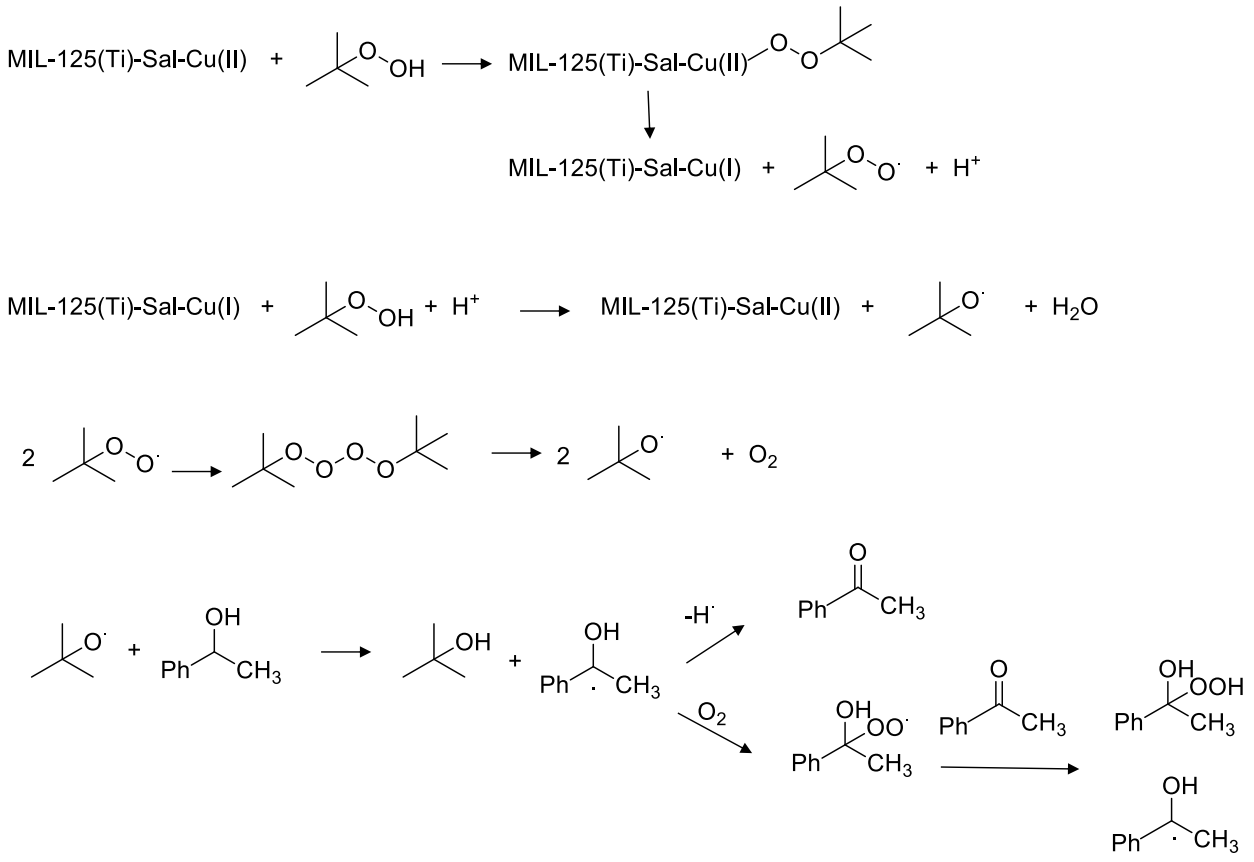

Scheme 2. Proposed reaction mechanism of 1-phenylethanol oxidation by ^{t}BuOOH promoted by Cu (II) in MIL-125(Ti)-NH_2-Sal-Cu (II).

The possible role of ambient molecular oxygen reacting with carbon centred radicals through a radical chain mechanism was studied by comparing the time conversion plots of 1-phenylethanol oxidation under air and under Ar atmosphere. The results (see Figure S5 in supporting information) show that the reaction rate is about 6 times faster in the presence of ambient oxygen than in its absence, indicating that, in this case, oxygen is enhancing the chain length by reacting with carbon centred radicals.

Another issue of interest is to provide evidence in support that the oxidation occurs inside MIL-125 (Ti)-NH_2 pores. To address this point, the catalytic activity of MIL-125(Ti)-NH_2-Sal-Cu was evaluated for the oxidation of *cis* and *trans* stilbene by TBHP. The results are shown in

Figure 11. While substitution in the two stilbene stereoisomers is similar, they possess a remarkable difference in molecular size and for these reason, these two isomers have been frequently used to assess shape-selectivity when the reaction is carried out inside pores. Thus, for instance, it has been found that while *trans*-stilbene can enter the pores of ZSM-5 and pentasil zeolites, the *cis* isomer is too large to enter the pores: The selective transformation of the *trans* isomer in the presence of *cis*-stilbene is one of the most remarkable shape-selectivity behavior reported for zeolites.[52]

As it can be seen in this Figure 11, a remarkable difference in stilbene conversion towards the corresponding epoxide depending on the configuration of the C=C double bond, the *trans* (much faster) versus the *cis* (slower) isomer, was experimentally observed. This distinctive reactivity is compatible with the occurrence of the reaction, at least partially, inside the pores. In this way, the higher reactivity of *trans*-stilbene would be a consequence of its faster diffusion through the pores, due to its smaller Lennard-Jones kinetic diameter compared (4.9 Å) to the bulkier cis isomer (7.8 Å).[53]

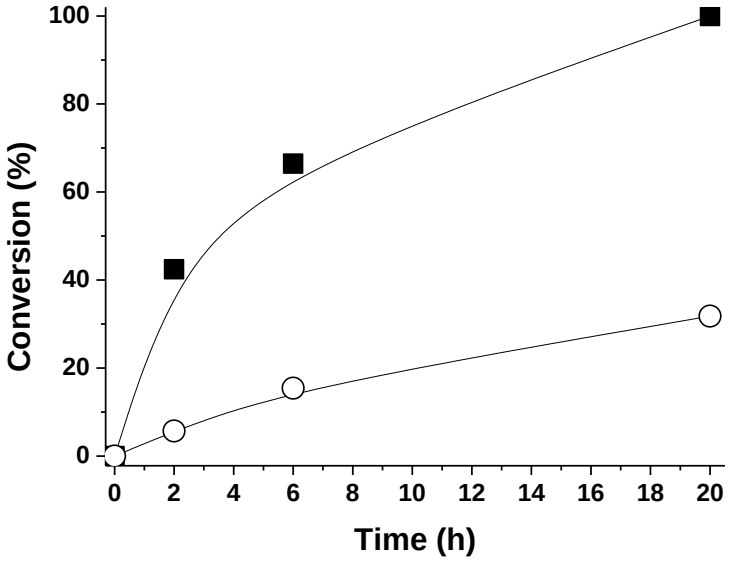

Figure 11. Time-conversion plot for the epoxidation of *trans*- (■) and *cis*- (○) stilbene catalyzed by MIL-125 (Ti)-NH_2-Sal-Cu. Reaction conditions: Catalyst (10 mg), substrate (1 mmol), CH_3CN (5 mL), TBHP (3 eq.) and 80 ºC.

The scope of the reaction using MIL-125(Ti)-NH_2-Sal-Cu as catalyst was screened by studying different substrates. The results are summarized in Table 2 and in Figure S6-S11. As it can be seen there, cyclohexene is selectively oxidized to cyclohexene oxide (22 %), cyclohexanol (55 %) and cyclohexanone (23 %) at 65 % conversion (Figure S6), resulting in a TOF of 360 h^{-1}. This value is about five times higher than the analogous MIL-53(Al)-NH_2-Sal Cu with the value of 73 h^{-1}.[39] In the case of benzyl alcohol, benzaldehyde is the primary oxidation product that undergoes subsequent oxidation to benzoic acid (Figure S7). Cyclic aliphatic alcohols, such as cyclohexanol, undergo also oxidation to the corresponding cyclic ketone, although in these cases higher molar ratio of TBHP respect to the substrate is needed to increase the conversion (Figure S8). Alternatively, cyclohexanol conversion can also be increased by using three equivalents of TBHP, but performing the reaction at higher temperature under oxygen pressure. Also under these harsher conditions stability of MIL-125(Ti)-NH_2-Sal-Cu was confirmed by XRD (see inset in Figure S8b.) Acyclic aliphatic alcohol, such as 1-octanol, are even more difficult to oxidize and conversions using 3 equivalents of TBHP its about 25 % conversion to give as reaction products a mixture of octanal and octanoic acid (Figure S9). As previously commented, conversion of 1-octanol was increased by performing the reaction at 100 ºC under 5 bar of oxygen pressure (Figure S10). These harsh conditions favor overoxidation of the substrate with higher selectivity towards octanoic acid versus octanal.

MIL-125(Ti)-NH_2-Sal-Cu is also a catalyst for the epoxidation of cyclooctene to cyclooctene oxide (Figure S11). This reaction is apparently more favorable and 2 equivalents of

TBHP are sufficient to achieve 100% cyclooctene conversion. A blank experiment using MIL-125(Ti)-NH_2 and MIL-125(Ti)-NH_2-Sal, show that these materials both without copper species produce also the epoxide, but with much slower kinetics and conversion at 24 h was only 20 % (Figure S11). This control indicates again that the Cu complex is acting as catalytic site for the epoxidation.

Table 2. Oxidation of different compounds using MIL-125 (Ti)-NH_2-Sal-Cu as catalyst.

	Time (h)	Conversion (%)	Main reaction products	Selectivity (%)
Cyclohexene	0.5	65	Cyclohexene oxide Cyclohexanol Cyclohexanone	22 55 23
Benzyl alcohol	1	18	Benzaldehyde Benzoic Acid	95 5
	24	92	Benzaldehyde Benzoic Acid	5 95
Cyclohexanol[a]	30	80	Cyclohexanone	>99
Cyclohexanol	30	60	Cyclohexanone	>99
Cyclohexanol[b]	5	72	Cyclohexanone	>99
1-Octanol	24	25	Octanal Octanoic Acid	40 60
1-Octanol[b]	28	40	Octanoic Acid	>99
Cyclooctene[c]	24	100	Cyclooctene oxide	>99
Ethylbenzene	24	60	Acetophenone	90

			Benzoic Acid	10
Ethylbenzene[b]	28	70	Acetophenone Benzoic Acid	10 90
Reaction condition: Catalyst (10 mg), substrate (1 mmol), CH_3CN (5 mL), TBHP (3 eq) and 80 ºC. [a] TBHP (5 eq), [b] 100 ºC, 5 bar O_2, TBHP (3 eq) and [c] TBHP (2 eq).				

MIL-125(Ti)-NH_2-Sal-Cu is also an efficient catalyst for the benzylic oxidation of ethylbenzene using 3 equivalents of TBHP at 80 ºC, reaching conversions of about 60 % at 24 h (Figure 12). The product formed was preferentially acetophenone, accompanied by lesser amounts of benzoic acid, although selectivity towards benzoic acid increases with conversion. To increase conversion, reaction conditions employing higher temperature under oxygen pressure were also tested, but only marginal conversion improvement could be achieved. It was observed, however, that harsher reaction conditions changes drastically the selectivity of the reaction in favor of the formation of benzoic acid that can be obtained finally with selectivity values closer to 90% (see Figure S12).

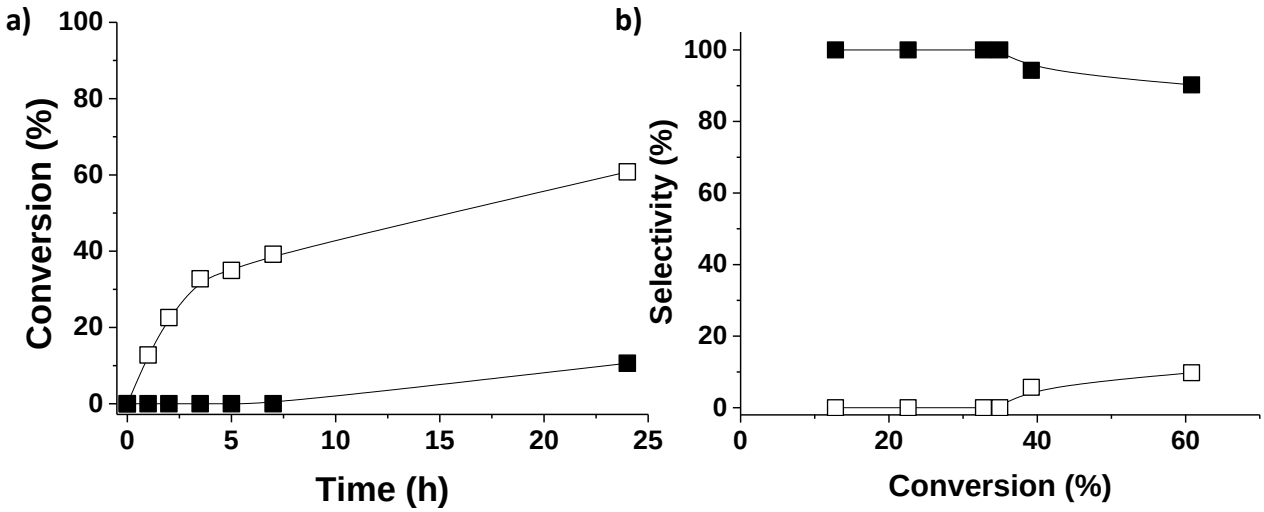

Figure 12. a) Time-conversion plot for the oxidation of ethylbenzene with TBHP using MIL-125(Ti)-NH_2-Sal-Cu (□), MIL-125(Ti)-NH_2 (■) **b)** Conversion-selectivity plot for acetophenone (■) and benzoic acid (□). Reaction conditions: Catalyst (10 mg), substrate (1 mmol), CH_3CN (5 mL), TBHP (3 eq.) and 80 ºC.

Conclusions

It has been shown that a Cu(II)-Shift base complex can be formed attached to satellite positions of MIL-125(Ti)-NH_2 framework by PSM based on the reactivity of the NH_2 substituents on the terephthalate linker.

The catalytic data obtained shows that these Cu-Sal complexes inside the pores of MIL-125 (Ti)-NH_2 exhibit catalytic activity for oxidation reactions with TBHP. This MIL-125 (Ti)-NH_2-Sal-Cu shows a broad scope promoting oxidation of benzylic, cyclic and linear aliphatic alcohols, as well as alkene epoxidation and benzylic oxidation. MIL-125(Ti)-NH_2-Sal-Cu (II) can be reused without any decay in its catalytic activity and without undergoing structural damage. Thus, all the available data obtained here or reported in the literature indicates that the catalytic ability of MIL-125(Ti)-NH_2-Sal-Cu to promote oxidations by TBHP is better than

homogeneous copper salts and complexes, particularly Cu-Sal, as well as other related heterogeneized catalysts in where Cu-Sal complexed had been attached to a solid support. This better performance appears to arise from the high porosity, surface area and immobilization of the Cu complex of the open framework of MOFs. Thus, our study illustrates again the potential that MOFs offers to anchor metallic complexes converting homogeneous catalysis into a heterogeneous process.

Acknowledgements

Financial support by the Spanish Ministry of Economy and Competitiveness (Severo Ochoa and CTQ2014-53292-R is gratefully acknowledged. Generalidad Valenciana is also thanked for funding (Prometeo 2017/063). S.D., A.R.O., D.A., and R.G-V thank H.G., S.N. and M.A.. S.D., D.A., and R.G-V gratefully acknowledge financial support from Bu-Ali Sina University. S.N. thanks financial support by the Fundación Ramón Areces (XVIII Concurso Nacional para la Adjudicación de Ayudas a la Investigación en Ciencias de la Vida y de la Materia, 2016).

References

(1) Férey, G. *Chem. Soc. Rev.* **2008**, *37*, 191-214.
(2) Furukawa, H.; Cordova, K. E.; O'Keeffe, M.; Yaghi, O. M. *Science* **2013**, *341*, 1230444.
(3) Kitagawa, S.; Kitaura, R.; Noro, S.-I. *Angew. Chem., Int. Ed.* **2004**, *43*, 2334-2237.
(4) Bai, Y.; Dou, Y.; Xie, L.-H.; Rutledge, W.; Li, J.-R.; Zhou, H.-C. *Chem. Soc. Rev.* **2016**, *45*, 2327-2367.
(5) Férey, G.; Serre, C.; Devic, T.; Maurin, G.; Jobic, H.; Llewellyn, P.; Weireld, G. D.; Vimont, A.; Daturi, M.; Chang, J.-S. *Chem. Soc. Rev.* **2011**, 550-562.
(6) Liu, J.; Thallapally, P. K.; McGrail, B. P.; Brown, D. R.; Liu, J. *Chem. Soc. Rev.* **2012**, *41*, 2308-2322.
(7) Farha, O. K.; Özgür Yazaydın, A.; Eryazici, I.; Malliakas, C. D.; Hauser, B. G.; Kanatzidis, M. G.; Nguyen, S. T.; Snurr, R. Q.; Hupp, J. T. *Nat. Chem.* **2010**, *2*, 944-948.
(8) Mason, J. A.; Veenstra, M.; Long, J. R. *Chem. Sci.* **2014**, *5* 32-51.
(9) Li, J.-R.; Sculley, J.; Zhou, H.-C. *Chem. Rev.* **2012**, *112*, 869-932.
(10) Van De Voorde, B.; Bueken, B.; Denayer, J.; De Vos, D. *Chem. Soc. Rev.* **2014**, *43*, 5766-5788.
(11) Bao, Z.; Chang, G.; Xing, H.; Krishna, R.; Ren, Q.; Chen, B. *Energy Environ. Sci.* **2016**, *9*, 3612-3641.
(12) Nasalevich, M. A.; Becker, R.; Ramos-Fernandez, E. V.; Castellanos, S.; Veber, S. L.; Fedin, M. V.; Kapteijn, F.; Reek, J. N. H.; van der Vlugt, J. I.; Gascon, J. *Energy Environ. Sci.* **2015**, *8*, 364-375.
(13) Chughtai, A. H.; Ahmad, N.; Younus, H. A.; Laypkov, A.; Verpoort, F. *Chem. Soc. Rev.* **2015**, *44*, 6804-6849.
(14) Corma, A.; García, H.; Llabrés I Xamena, F. X. *Chem. Rev.* **2010**, *110*, 4606-4655.
(15) Fang, Z.; Bueken, B.; De Vos, D. E.; Fischer, R. A. *Angew. Chem Int. Ed.* **2015**, *54*, 7234-7254.
(16) Farrusseng, D.; Aguado, S.; Pinel, C. *Angew. Chem., Int. Ed.* **2009**, *48*, 7502-7513
(17) Liu, J.; Chen, L.; Cui, H.; Zhang, J.; Zhang, L.; Su, C.-Y. *Chem. Soc. Rev.* **2014**, *43*, 6011-6061.
(18) Rogge, S. M. J.; Bavykina, A.; Hajek, J.; Garcia, H.; Olivos-Suarez, A. I.; Sepúlveda-Escribano, A.; Vimont, A.; Clet, G.; Bazin, P.; Kapteijn, F.; Daturi, M.; Ramos-Fernandez, E. V.; Llabrés i Xamena, F. X.; Van Speybroeck, V.; Gascon, J. *Chem. Soc. Rev.* **2017**, *46*, 3134-3184.
(19) Yoon, M.; Srirambalaji, R.; Kim, K. *Chem. Rev.* **2012**, *112*, 1196-1231.
(20) Ghorbani-Vaghei, R.; Davood, A.; Daliran, S.; Oveisi, A. R. *RSC Adv.* **2016**, *6*, 29182-29189.
(21) Ji, P.; Manna, K.; Lin, Z.; Feng, X.; Urban, A.; Song, Y.; Lin, W. *J. Am. Chem. Soc.* **2017**, *139*, 7004-7011.
(22) Oveisi, A. R.; Khorramabadi-zad, A.; Daliran, S. *RSC Adv.* **2016**, *6*, 1136-1142.
(23) Rimoldi, M.; Howarth, A. J.; DeStefano, M. R.; Lin, L.; Goswami, S.; Li, P.; Hupp, J. T.; Farha, O. K. *ACS Catal.* **2017**, *7*, 997-1014.
(24) Kreno, L. E.; Leong, K.; Farha, O. K.; Allendorf, M.; Van Duyne, R. P.; Hupp, J. T. *Chem. Rev.* **2012**, *112*, 1105-1125.
(25) Horcajada, P.; Gref, R.; Baati, T.; Allan, P. K.; Maurin, G.; Couvreur, P.; Férey, G.; Morris, R. E.; Serre, C. *Chem. Rev.* **2012**, *112*, 1232-1268.
(26) Dhakshinamoorthy, A.; Asiri, A. M.; García, H. *Angew. Chem Int. Ed.* **2016**, *55*, 5414-5445
(27) Bobbitt, N. S.; Mendonca, M. L.; Howarth, A. J.; Islamoglu, T.; Hupp, J. T.; Farha, O. K.; Snurr, R. Q. *Chem. Soc. Rev.* **2017**, *46*, 3357-3385.
(28) Cohen, S. M. *Chem. Rev.* **2012**, *112*, 970-1000.
(29) Cohen, S. M. *J. Am. Chem. Soc.* **2017**, *8*, 2855-2863.
(30) de Miguel, M.; Ragon, F.; Devic, T.; Serre, C.; Horcajada, P.; García, H. *ChemPhysChem* **2012**, *13*, 3651-3654.
(31) Hu, S.; Liu, M.; Li, K.; Zuo, Y.; Zhang, A.; Song, C.; Zhang, G.; Guo, X. *CrystEngComm.* **2014**, *16*, 9645-9650.

(32) Vaesen, S.; Guillerm, V.; Yang, Q.; Wiersum, A.; Marszalek, B.; Gil, B.; Vimont, A.; Daturi, M.; Devic, T.; Llewellyn, P. L.; Serre, C.; Maurin, G.; Weireld, G. D. *Chem. Comm.* **2013**, *49*, 10082-10084.
(33) Zhang, Y.; Chen, Y.; Zhang, Y.; Cong, H.; Fu, B.; Wen, S.; Ruan, S. *J. Nanopart. Res.* **2013**, *15*, 2014.
(34) Chambers, M. B.; Wang, X.; Ellezam, L.; Ersen, O.; Fontecave, M.; Sanchez, C.; Rozes, L.; Mellot-Draznieks, C. *J. Am. Chem. Soc.* **2017**, *139*, 8222-8228.
(35) Logan, M. W.; Lau, Y. A.; Zheng, Y.; Hall, E. A.; Hettinger, M. A.; Marks, R. P.; Hosler, M. L.; Rossi, F. M.; Yuan, Y.; Uribe-Romo, F. J. *Catal. Sci. Technol.* **2016**, *6*, 5647-5655.
(36) Ivanchikova, I. D.; Lee, J. S.; Maksimchuk, N. V.; Shmakov, A. N.; Chesalov, Y. A.; Ayupov, A. B.; Hwang, Y. K.; Jun, C.-H.; Chang, J.-S.; Kholdeeva, O. A. *Eur. J. Inorg. Chem.* **2014**, 132-139.
(37) Kim, S.-N.; Kim, J.; Kim, H.-Y.; Cho, H.-Y.; Ahn, W.-S. *Catal. Today* **2013**, *204*, 85-93.
(38) McNamara, N. D.; Neumann, G. T.; Masko, E. T.; Urban, J. A.; Hicks, J. C. *J. Catal.* **2013**, *305*, 217-226.
(39) Bunchuay, T.; Ketkaew, R.; Chotmongkolsap, P.; Chutimasakul, T.; Kanarat, J.; Tantirungrotechai, Y.; Tantirungrotechai, J. *Catal. Sci. Technol.* **2017**, *7*, 6069-6079.
(40) López-Santos, C.; Yubero, F.; Cotrino, J.; González-Elipe, A. R. *Diamond Relat. Mater.* **2011**, *20*, 49−56.
(41) Dan-Hardi, M.; Serre, C.; Frot, T.; Rozes, L.; Maurin, G.; Sanchez, C.; Ferey, G. *J. Am. Chem. Soc.* **2009**, *131*, 10857-10859.
(42) Azarifar, D.; Ghorbani-Vaghei, R.; Daliran, S.; Oveisi, A. R. *ChemCatChem.* **2017**, *9*, 1992-2000.
(43) Houa, J.; Luana, Y.; Tanga, J.; Wensleya, A. M.; Yanga, M.; Lub, Y. *J. Mol. Catal. A.* **2015**, *407*, 53-59.
(44) Audu, C. O.; Nguyen, H. G. T.; Chang, C.-Y.; Katz, M. J.; Mao, L.; Farha, O. K.; Hupp, J. T.; Nguyen, S. T. *Chem. Sci.* **2016**, *7*, 6492-6498.
(45) Zwoliński, K. M.; Nowak, P.; Chmielewski, J. *Chem. Commun.* **2015**, *51*, 10030-10033.
(46) Wang, H.; Yuan, X. Y.; Wu, Y.; Zeng, G.; Chen, X.; Leng, L.; Wu, Z.; Jiang, L.; Li, H. *J. Hazard. Mater.* **2015**, *286*, 187-194.
(47) Allen, S. E.; Walvoord, R. R.; Padilla-Salinas, R.; Kozlowski, M. C. *Chem. Rev.* **2013**, *113*, 6234-6458.
(48) Navalón, S.; Herance, J. R.; Álvaro, M.; GarcIa, H. *Chem. Eur. J.* **2017**, *23*, 15244 – 15275.
(49) Verma, S.; Nandi, M.; Modak, A.; Jain, S. L.; Bhaumik, A. *Adv. Synth. Catal. 2011, ,* **2011**, *353*, 1897 - 1902.
(50) Ferguson, G.; Ajjou, A. N. *Tetrahedron Lett.* **2003**, *44*, 9139-9142.
(51) Paavola, S.; Zetterberg, K.; Privalov, T.; Csˆregh, I.; Moberg, C. *Adv. Synth. Catal. 2004, ,* **2004**, *346*, 237 - 244.
(52) Baldoví, M. V.; Corma, A.; García, H.; Martí, V. *Tetrahedron Lett.* **1994**, 9447-9450.
(53) Metin, O.; Alcan Alp, N.; Akbayrak, S.; Biçer, A.; Serdar Gültekin, M. S.; zkar, S.; Bozkaya, U. *Green Chem.* **2012**, *14*, 1488-1492.